

Finite temperature properties of the 2D Kondo lattice model

K. Haule^a, J. Bonča^{a,b} and P. Prelovšek^{a,b}

^a *J. Stefan Institute, Ljubljana*, ^b *FMF, University of Ljubljana Slovenia*
(October 23, 2018)

Using recently developed Lanczos technique we study finite-temperature properties of the 2D Kondo lattice model at various fillings of the conduction band. At half filling the quasiparticle gap governs physical properties of the chemical potential and the charge susceptibility at small temperatures. In the intermediate coupling regime quasiparticle gap scales approximately linearly with Kondo coupling as $\Delta_{qp}/J \sim 0.3$. Temperature dependence of the spin susceptibility reveals the existence of two different temperature scales. A spin gap in the intermediate regime leads to exponential drop of the spin susceptibility at low temperatures. Unusual scaling of spin susceptibility is found for temperatures above $T_c \geq 0.6J$. Charge susceptibility at finite doping reveals existence of heavy quasiparticles. A new low energy scale is found at finite doping.

pacS-71.10.-w 71.27.+a 65.50.+m

I. INTRODUCTION

The Kondo lattice model is one of the simplest two-band lattice models of correlated electrons. It is widely used to model heavy fermion materials where weakly interacting electrons in wide bands coexist with almost localized electrons in unfilled orbitals of actinide or rare-earth elements. In heavy fermion materials a remarkable variety of different phases can be found at low temperatures: paramagnetic metal with large quasiparticle mass, anti-ferromagnetic and ferromagnetic phases, unconventional superconductivity, etc. In most of these cases, strong electron correlations represent the key ingredient of the theory that explains the rich variety of physical phenomena.

In this work we investigate the Kondo lattice model, defined on small two dimensional square lattices with periodic boundary conditions. We use the finite-temperature Lanczos method [1]. The model can be written as

$$H = -t \sum_{\langle \mathbf{ij} \rangle_s} c_{i\mathbf{s}}^\dagger c_{j\mathbf{s}} + \text{H.c.} + J \sum_{\mathbf{i}} \mathbf{S}_i \mathbf{S}_i \quad (1)$$

where $\mathbf{S}_i = \sum_{ss'} c_{is'}^\dagger \sigma_{s's} c_{is}$ and summation $\langle \mathbf{ij} \rangle$ runs over nearest neighbors. There are two distinct types of degrees of freedom in this model: free electrons described by c operators and localized spins described by \mathbf{S} . In the limit when $J = 0$ the two systems are decoupled which leads to a large degeneracy of the states due to noninteracting spins. At finite Kondo coupling $J \neq 0$ the two systems interact. It is believed, that the interplay between the two degrees of freedom represents the most important physical mechanism of the heavy Fermion materials. Associated with the two distinct systems are two competing interactions that govern the low-temperature physics. Finite Kondo coupling leads to formation of Kondo spin-singlets between the conducting electrons and the localized spins which screens the moments of

localized spins. Singlet formation competes with band propagation of electrons in the conduction band. Coupling between kinetic energy of band electrons and local Kondo coupling leads to formation of the Ruderman-Kittel-Kasuya-Yoshida (RKKY) interaction between localized spins. The Kondo screening on the one hand and the RKKY interaction on the other are in many cases competing interactions. Conditions, under which one or the other prevails depend mostly on the strength of the Kondo coupling, the electron filling and the dimensionality of the system.

A number of theoretical approaches has been applied to the investigation of the Kondo lattice model [2]. In the strong coupling regime perturbation theory can be applied [3]. Large- N_f expansion can be used in the case of large localized spin-degeneracy N_f [4]. Slave-boson approach [4], Gutzwiller variational treatments [5] and recently developed strong coupling method [6] have been successful in predicting the heavy mass of the quasiparticles, the phase diagram and the properties of the spectral functions.

Numerical calculations have been mostly limited to one dimensional systems where various well developed techniques are available and finite-size effects can be easily controlled. Calculations on small systems have demonstrated that at half-filling the one dimensional Kondo lattice model is a spin-liquid with a finite spin gap [7]. Density-matrix numerical-renormalization group (DMRG) calculations [8], provided accurate determination of the spin and charge gaps as a function of the Kondo coupling [9,10]. Recently, a powerful finite-temperature DMRG method [11,12] have provided reliable results for thermodynamic [13–15] and dynamic properties [15,16] of the model at $T > 0$.

While there are many reliable numerical results of the Kondo lattice model in 1D, much less is known about the model in two or three dimensions. Based on theoretical considerations conceptually different physical behavior is expected in higher dimensions. Spin-charge separation

exists in 1D models as a consequence of strong correlations. It is reflected in different energy scales that govern the low-energy behavior of spin and charge excitations leading to a difference between the spin and the charge velocities. Luttinger liquid parameters define power-law behavior of correlation functions in 1D while in higher dimensions exponential behavior of correlation functions is expected unless long-range order exists. The lack of long-range order in 1D is responsible for Kondo screening to overcome the RKKY interaction for any finite J . In two dimensions there exists a critical value of $J_c/t \sim 1.4$ [17–19] below which RKKY interaction prevails and system orders antiferromagnetically in the case when the conduction band is half filled.

The main purpose of this work is to explore thermodynamic properties of the 2D Kondo lattice model. We focus our investigations to intermediate and high temperatures and try to identify various energy and temperature scales that govern the spin and the charge response of the system. Due to small system size we are not able to explore extremely low temperatures since in this regime strong finite-size effects emerge. For the same reason we limit our calculations to intermediate and strong coupling regime where physics is sufficiently local so that our results remain valid even in the thermodynamic limit.

II. RESULTS

Our numerical calculations are performed by recently developed finite-temperature Lanczos method [1]. We investigate square lattices of $N = 8$ and 10 sites. Most of the results presented are for the $N = 10$ case. Standard zero-temperature exact diagonalization results on small clusters are generally plagued by strong finite-size effects. Performing calculations at finite temperatures and within the grand-canonical ensemble gives us not only the thermodynamical properties of the system, but most importantly diminishes finite-size effects for $T > T^*$ [1]. This temperature depends primarily on the number of low lying excited states in the system. The T^* can be very small when the system possesses either: a) a large number of low-lying energy states, or b) if physics is sufficiently local. Local physics is expected at large Kondo coupling where the size of the Kondo singlet is of the order of a few lattice spacings. We present results for half-filled conduction band case $n_c = 1$ and at finite doping δ defined by $n_c = 1 - \delta$. Due to particle-hole symmetry only $\delta > 0$ is considered. In this work we restrict calculations to thermodynamic quantities as are the chemical potential μ , spin susceptibility $\chi_s = \langle S_{tot}^z{}^2 \rangle / T$, charge susceptibility $\chi_c = -d\delta/d\mu = (\langle n_c^2 \rangle - \langle n_c \rangle^2) / T$ and the specific heat $c_v = -T\partial^2 F / \partial T^2$. Despite small system size we can compute thermodynamic quantities at any doping δ simply by choosing the appropriate chemical potential [1].

A. The chemical potential μ

In Fig. (1a) we show chemical potential μ as a function of temperature for small doping values and $J/t = 2.5$. Due to particle-hole symmetry the relation $\mu(\delta = 0) = 0$ is valid at any temperature. At high temperature and finite doping the chemical potential approaches a simple expression (faint dotted lines), calculated by the finite-temperature expansion

$$\mu = T \left(\log \frac{1 - \delta}{1 + \delta} - \frac{\delta}{2T^2} \left(\frac{3J^2}{8} + 8t^2 \right) \right). \quad (2)$$

While the first term is model independent, the second term represents the first nontrivial finite-temperature correction. Numerical results start deviating significantly from the high-temperature expression below $T/t \sim 2$. At small temperatures chemical potential approaches a finite value even in the limit $\delta \rightarrow 0$. Infinitesimally small doping away from the half-filled conduction band leads to an abrupt change of the chemical potential. Such behavior indicates formation of the quasiparticle gap Δ_{qp} also found in the 1d DMRG calculations [14]. To investigate the quasiparticle gap in more detail, we present in Fig.(1b) μ/J at fixed doping for different choices of the Kondo coupling strength on a system of $N = 10$ sites. We find that the quasiparticle gap increases almost linearly with the Kondo coupling J in the intermediate coupling range, *i.e.* for $J/t = 1.6, 2.0$ and 2.5 . Extrapolated values of the quasiparticle gap in the limit $T \rightarrow 0$ are presented in table (I) for systems of $N = 8$ and 10 sites. Results, obtained from the two systems agree reasonably well in the intermediate coupling range. The lack of finite-size effects in the limit when $T \rightarrow 0$ is attributed to the existence of the quasiparticle gap. Near the strong coupling limit, $J/t = 10$, the extrapolated values for the quasiparticle gap agree well with the strong coupling result $\Delta_{qp} = \frac{3}{4}J - 2t + \frac{13}{6}t^2/J = 5.72$ [2].

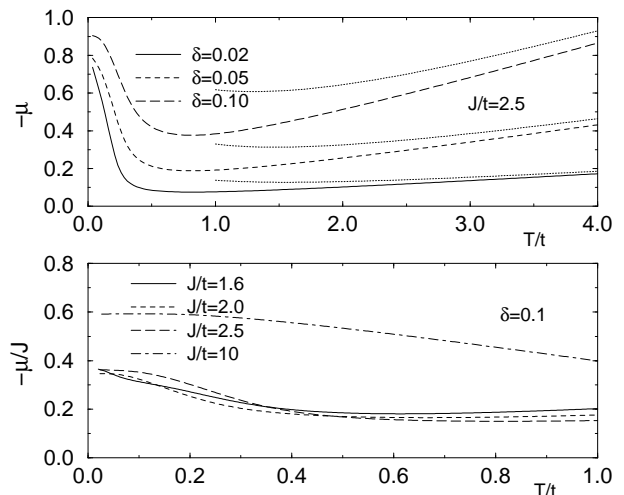


FIG. 1. Chemical potential μ as a function of temperature T ; a) at different dopings δ and fixed J , b) at fixed doping δ and different couplings J/t .

B. Spin and charge susceptibilities

1. Strong coupling (atomic) limit

At large values of Kondo coupling, $J/t = 10$, physics of the Kondo model becomes local. We support our claim by results shown in Fig. (2) where we present comparison of spin (and charge) susceptibility for $J/t = 10$ and analytical results obtained within the atomic limit of the Kondo model. In this limit the grand canonical sum can be calculated as $Z = \sum_{j=1}^8 e^{-\beta(E_j^{at} - \mu N)}$, where β is the inverse temperature and only 8 states are taken into account: the singlet state with the energy $E_{S=0}^{at} = -3J/4$, the three-fold degenerate triplet state $E_{S=1}^{at} = J/4$ both containing one conduction electron and four-fold degenerate states $E_{S=1/2}^{at} = 0$ consisted of an empty and a doubly occupied conduction level each of them with two different spin configurations. Values of spin, quasiparticle and charge gap are in this limit given by $\Delta_s/J = 1$, $\Delta_{qp}/J = 3/4$, and $\Delta_c/J = 1.5$. At zero doping ($\delta = 0$) spin and charge susceptibility are given by simple expressions

$$\chi_s = \beta \frac{1 + 2e^{-\beta J/4}}{4 + 3e^{-\beta J/4} + e^{3\beta J/4}}, \quad (3)$$

$$\chi_c = \beta \frac{4}{4 + 3e^{-\beta J/4} + e^{3\beta J/4}}, \quad (4)$$

where β is the inverse temperature and $\mu = 0$. Susceptibility, Eq. (4) presented in Fig. (2) follow $1/T$ law at high temperatures. At lower temperatures we see a peak, marked by arrows. We introduce two temperature scales that mark the peak positions: $T_s/J = 0.453$ and $T_{qp}/J = 0.386$ for spin and charge susceptibility respectively. Given values were obtained analytically. At low temperatures both susceptibilities approach zero at $\delta = 0$ which is consistent with the existence of a gap in the excitation spectrum. Low-temperature behavior is in both cases given by $\chi_{c,s} \propto \beta \text{Exp}[-3\beta J/4]$ which leads us to a conclusion, that the quasiparticle (smallest) gap $\Delta_{qp}/J = 3/4$ governs the low-temperature behavior of both susceptibilities. This is possible since a quasiparticle excitation modifies the charge configuration and also changes the spin quantum number by $\pm 1/2$. Even though both susceptibilities share a common gap, they reach a maximum at slightly different temperatures T_s and T_{qp} which is due to different nature of the excitation spectra above the gap.

We see that numerical calculations at large $J/t = 10$, also presented in Fig. (2), agree reasonably well with analytical results at zero and finite doping. Agreement at finite doping is somewhat surprising since in the atomic

limit only a single site of the Kondo lattice is taken into account. To understand the divergence of spin and charge susceptibilities at low temperatures and finite doping, we perform low-temperature expansion which gives us

$$\mu = -\frac{3}{4}J + T \ln \left(\frac{2(1-\delta)}{\delta} \right), \quad (5)$$

$$\chi_s = \frac{\delta}{4T}, \quad (6)$$

$$\chi_c = \frac{\delta(1-\delta)}{T}. \quad (7)$$

Divergence at low temperatures is in the strong coupling regime a consequence of a degenerate level system. At even lower temperatures, numerical results should saturate towards finite values in both cases, the spin and the charge susceptibility. In the later case a deviation from the predicted $1/T$ law can be seen in Fig. (2b) while in the former case such deviation is expected at even lower temperatures.

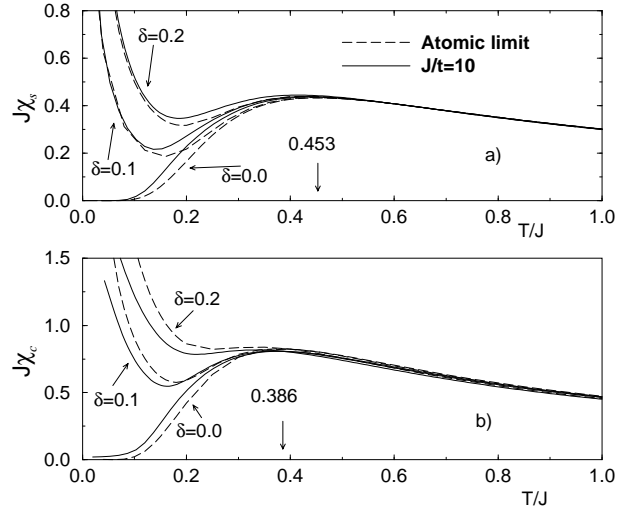


FIG. 2. Spin a) and charge b) susceptibilities χ_s, χ_c vs. T/J calculated numerically at $J/t = 10$ (full lines). Dashed curves represent results obtained in the atomic limit. Positions of the peaks T_s in a) and T_{qp} in b) in the atomic limit and zero doping are indicated with arrows.

2. Zero doping

In Fig. (3a) we present spin susceptibilities $J\chi_s(T/J)$ at zero doping, $\delta = 0$ for different values of the Kondo interaction J . At high temperature ($T > J$) numerical results agree with the high-temperature expansion,

$$\chi_s = \frac{3 - \delta^2}{8T} \left[1 - \frac{1 - \delta^2}{3 - \delta^2} \frac{J}{2T} \right], \quad (8)$$

performed to the first nontrivial order. In the intermediate temperature regime we find rather surprising result.

All curves merge on a single curve for $T/J > T_c/J \sim 0.6$. It could be argued that this is because the high-temperature result in Eq. (8) scales with J , *i.e.* the function $J\chi_s(J/T)$ is independent of J . However, the agreement with the Eq. (8) is only within 10% up to $T/J \sim 1$ (see Fig. (3a)) while the overlap of susceptibilities calculated for a wide range of J/t is within a few percents. At low temperature, spin susceptibility reaches a maximum at $T = T_s$ and then approaches zero. In the strong coupling limit spin gap is larger than the quasiparticle gap however at smaller J/t this is no longer true. In the region of small $J/t \sim 1.4$ spin gap approaches zero due to formation of AFM order [19]. Low temperature behavior of spin susceptibility in the intermediate coupling regime is thus governed by the spin gap. There are two possible approaches to estimate the spin gap using our method. In the zero-temperature approach the spin gap equals the energy difference between the lowest ($S = 0$) and the first excited ($S = 1$) state. At finite temperature, the spin gap is roughly proportional to the position of the peak in $\chi_s(T)$ given by the activation temperature T_s . We believe, that the second method, even though indirect, gives results that are closer to the thermodynamic limit.

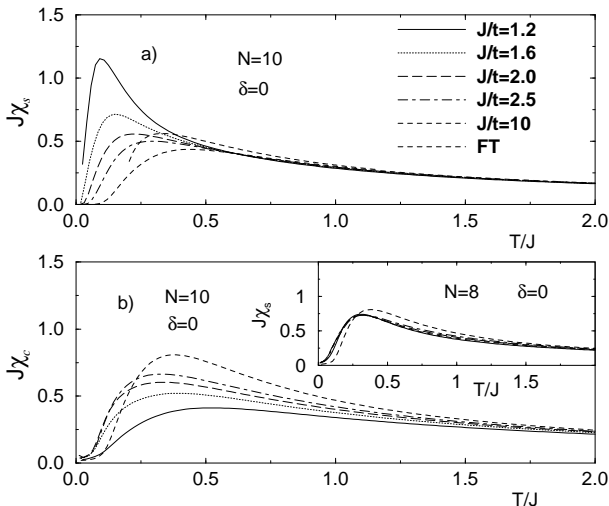


FIG. 3. Spin a) and charge b) susceptibilities $J\chi_s$, $J\chi_c$ vs. T/J at zero doping. Faint dashed line in a) represent high-temperature expansion result, Eq. (8). Legends, given in a) apply also for b) and the inset in b). In the inset in b) all six different curves for $J/t = 1.2 \dots 10$ are presented. All, except for $J/t = 10$ appear as a single line. Legend FT in a) indicates analytical result in Eq. (8).

Values of T_s are presented in Table (I). As seen from Fig. (3a) with increasing coupling J , low-temperature peak in spin susceptibility moves toward higher values of T/J . T_s therefore does not scale linearly with J for small J as does the quasiparticle gap (see also Table (I)). This points towards a non-linear dependence of spin-gap

vs. J/t that is found in one-dimensional system [2] and also recent calculations in the 2D system [19]. A qualitatively good agreement is also found between T_s and the spin gap obtained by the projection quantum Monte Carlo simulations [19].

At small values of the Kondo coupling $J/t < 1.4$ gapless AFM long range order develops on an infinite lattice as a consequence of RKKY interaction [18,19]. Uniform spin susceptibility in this case saturates around the temperature which is given by the RKKY interaction between localized spins. Our results in this regime become less reliable at low temperature due to strong finite-size effects.

The charge susceptibility χ_c shows in sharp contrast to the strong coupling limit in many respects different behavior than the spin susceptibility. Starting from the high-temperature limit we first present the high-temperature result for the charge susceptibility

$$\chi_c = \frac{1 - \delta^2}{2T} \left[1 - \frac{1 + \delta^2}{8T^2} \left(\frac{3J^2}{8} + 8t^2 \right) \right]. \quad (9)$$

Note that in contrast to spin susceptibility, the first non-trivial correction in the inverse temperature is $1/T^3$. The agreement of numerical results with the high-temperature expansion strongly depends on J . In Fig. (3b) we show $J\chi_c(T/J)$ at zero doping and a wide range of J . At large $J/t = 10$, where J is the dominant energy scale in the system, numerical results agree with the analytical result, given by Eq. (9), down to $T/J = 0.4$. At smaller J high-temperature limit is reached above $T/J > 2$.

The charge susceptibility is governed by a single energy scale, *i.e.* the quasiparticle gap Δ_{qp} . This is reflected in nearly perfect scaling of $J\chi_c(T/J)$ for the $N = 8$ system in the intermediate coupling region $1.2 \leq J/t \leq 2.5$ (see the inset of Fig. (3b)). Scaling is due to the fact that the quasiparticle gap scales nearly linearly with J , *i.e.* $\Delta_{qp} \simeq 0.3J$ in this regime. The quasiparticle gap remains finite even at small $J \sim 1.2$ where the spin gap disappears. The scaling does not persist up to the strong coupling limit, $J/t = 10$ due to a crossover regime where the spin gap becomes larger than the quasiparticle gap. The location of the peak at $T = T_{qp}$ seen in the temperature dependence of the charge susceptibility curves matches the value of the quasiparticle gap $T_{qp} = \Delta_{qp}$ obtained from measurements of the doping dependence of the chemical potential (see table (I)). Despite a smaller system size we believe, that near or at zero doping, $N = 8$ system shows less finite-size effects than the $N = 10$ when calculating quasiparticle properties of the system. The reason is that the $N = 8$ noninteracting fermion system has a six-fold degenerate level at zero energy which overlaps with the value of the chemical potential at zero doping. In contrast, the $N = 10$ noninteracting system has a large gap at μ . The scaling is therefore less obvious for the $N = 10$ system size, however locations of

the peaks nevertheless approximately scale with J and peak positions T_{qp} approximately match the quasiparticle gaps obtained from the chemical potential curves for $J = 1.6, 2.0$, and 2.5 .

3. Finite doping

Spin and charge susceptibilities, presented in Fig. (4a), at small doping $\delta = 0.1$ show similar high-temperature behavior as in the zero doping case. At high-temperature, χ_s follows Curie-like $1/T$ behavior, predicted by the high-temperature expansion given by Eq. (8). As in the zero-doping case, susceptibility curves calculated for different J/t show scaling above $T/J > T_c/J \sim 0.6$. With decreasing temperature χ_s reaches a peak at $T = T_s$ where T_s is close to its $\delta = 0$ value. Even though the spin gap disappears at finite doping and zero temperature, at finite temperature remains of the spin gap can be observed even at finite doping. Similar results were observed in one-dimensional calculations [14]. With further decreasing of the temperature χ_s first decreases and then sharply increases at even lower temperature. In this region the susceptibility curve can be fitted to a simple form $\chi_s = \delta C/T$. This Curie-like form suggests that finite doping produces nearly free localized spins. In contrast to one-dimensional results [14], we found that for intermediate values of the Kondo coupling $J/t = 1.6, 2.0$ and 2.5 the local moment is reduced and equals $C \sim 0.18$. In the strong coupling limit, $J/t = 10$, the local moment reaches its maximum value $C = 0.25$. In the extreme low-temperature limit spin susceptibility should saturate either due to RKKY interaction between localized spin for small values of J/t or due to Kondo screening effects for larger J/t . This effect can be seen in the case of larger doping, $\delta = 0.2$, where for intermediate Kondo coupling, *i.e.* $J/t = 1.6, 2.0$ and 2.5 susceptibility curves show less divergent behavior as in the $\delta = 0.1$ case.

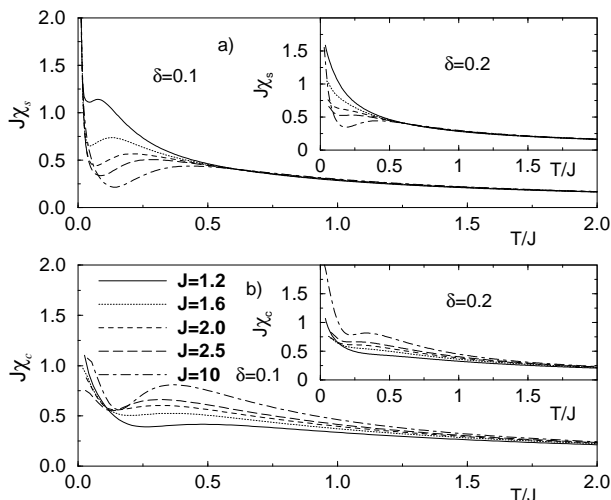


FIG. 4. Spin a) and charge b) susceptibilities $J\chi_s$, $J\chi_c$ vs. T/J at $\delta = 0.1$ and 0.2 . Legends, given in b) apply also for a) and both insets.

The charge susceptibility at $\delta = 0.1$, presented in Fig. (4b), follows $1/T$ behavior at high-temperature, predicted by the high-temperature expansion given by Eq. (9). Susceptibility reaches a local maximum around $T = T_{qp}$. For small doping T_{qp} overlaps with its value at $\delta = 0$. At even smaller temperature we observe a sharp increase in χ_c . At zero-temperature charge susceptibility should equal the density of states at the Fermi energy which is further proportional to the quasiparticle mass. The sharp increase of χ_c therefore suggests that quasiparticles are massive.

C. Specific heat

Results for the specific heat c_v are shown in Fig. (5) for various values of J/t . In Fig. (5a) we show c_v as a function of T/t . At $J/t = 0$, c_v has a peak at finite temperatures which originates from the specific heat of free conduction electrons. The contribution of localized noninteracting spins is nonanalytic and proportional to $T\delta(T)$ where $\delta(x)$ is a delta-function. At small values of Kondo coupling, *e.g.* $J/t = 0.8, 1.2, 1.6$ and 2.0 we observe two peaks in the specific heat. The low-temperature peak that has emerged from the nonanalytic function at $J/t = 0$ is a contribution of the spin excitations. With increasing J/t it shifts towards higher temperatures and broadens. The broadening is due to the spin excitation spectrum that has a bandwidth of some effective J_{eff} which increases with the strength of the Kondo coupling. The broad peak, that originated from the free electron band at $J/t = 0$, shifts towards higher temperatures with increasing J/t and becomes even broader. This is due to the interplay of band effects and the charge gap that develops with increasing J/t . The two peaks above $J/t = 2.5$ merge into a single peak which in the strong coupling limit scales linearly with J . At $J/t = 10$ specific heat closely follows analytical prediction calculated within the atomic limit as seen in Fig. (5b) where c_v is presented as a function of T/J . Our results for the two-dimensional lattice are in many respects similar to results for the one-dimensional lattice obtained by the DMRG method [13,15].

III. CONCLUSIONS

We have investigated finite-temperature properties of the Kondo lattice model on small square lattices. The chemical potential at low temperatures shows nonanalytic behavior as a function of doping. The jump in the chemical potential is a consequence of the quasiparticle gap at zero doping. The quasiparticle gap scales approximately linearly with the Kondo coupling, $\Delta_{qp} \sim 0.3J$ in the intermediate coupling regime, *i.e.* $1.6 \leq J/t \leq 2.5$. Similar scaling was recently found by quantum Monte Carlo simulations [19] which furthermore show that scaling persists even below the transition to the AFM state, *i.e.* $J/t \sim 1.4$. In the strong coupling regime the quasiparticle gap again scales linearly with J as $\Delta_{qp} \sim 0.75J$ which is not too surprising since in this case physics becomes local and J is then the only energy scale in the system. The crossover between the two linear regimes occurs when the spin gap overcomes the quasiparticle gap, *i.e.* at $J/t > 2.5$. Interestingly, calculations in one dimension show two distinct linear regimes for the charge gap vs. J/t [10].

Two temperature scales govern the temperature dependence of spin susceptibility in the intermediate coupling regime. One scale is given by $T_c/J \sim 0.6$ above which we find almost perfect scaling of curves calculated for a wide range of coupling strengths J . One possible explanation of this unusual scaling is that T_c is governed by the charge gap Δ_c . We have shown in the previous section that the quasiparticle gap at intermediate coupling scales linearly with J as $\Delta_{qp} \sim 0.3J$. Assuming $\Delta_c = 2\Delta_{qp}$ we get a linear scaling for the charge gap, $\Delta_c \sim 0.6J$, which agrees with the value for T_c . At lower temperatures, $T \sim T_s$, physics at zero doping is governed by the spin gap Δ_s . This remains true as long as $\Delta_s < \Delta_{qp}$. Near the strong coupling regime the opposite becomes true, then the quasiparticle gap determines the low-temperature physics of the spin susceptibility.

The charge susceptibility shows substantially different behavior than the spin susceptibility. On a smaller system of $N = 8$ we found almost perfect scaling with J in the whole temperature range within the intermediate Kondo coupling region. This result suggests that a single energy scale, identified as a quasiparticle gap $\Delta_{qp} \sim 0.3J$, governs the physics of the charge response of the system.

At finite doping we found a new energy scale. It is reflected in the saturation of divergent $1/T$ behavior in $\chi_s(T)$ at small temperatures and in the appearance of low-temperature peaks in the specific heat c_v at $\delta = 0.2$. Approximate quadratic scaling of the position of the peaks in c_v with the Kondo coupling strength suggests, that this energy scale could be attributed to the RKKY interaction between uncompensated spins at finite doping.

One of the authors, J.B. is grateful for the hospitality

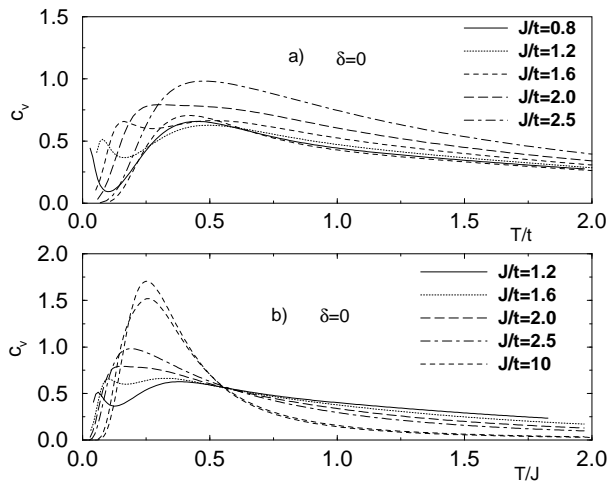


FIG. 5. Specific heat at $\delta = 0$ c_v a) vs. T/t and b) vs. T/J calculated on a system of $N = 10$. The faint dashed line represents the free electron result a) and result obtained in the atomic limit b).

At finite doping, $\delta = 0.1$ shown in Fig. (6a), small peaks due to the spin gap are still visible at small temperatures. At even larger doping, $\delta = 0.2$ shown in Fig. (6b), new peaks emerge at very small temperatures (see also the inset of Fig. (6b)). This peaks shift towards larger temperatures with increasing Kondo coupling. The shift is approximately quadratic in J . We believe that the same low energy scale that gives rise to these peaks is responsible for saturation of spin susceptibility seen in the intermediate coupling J/t and $\delta = 0.2$.

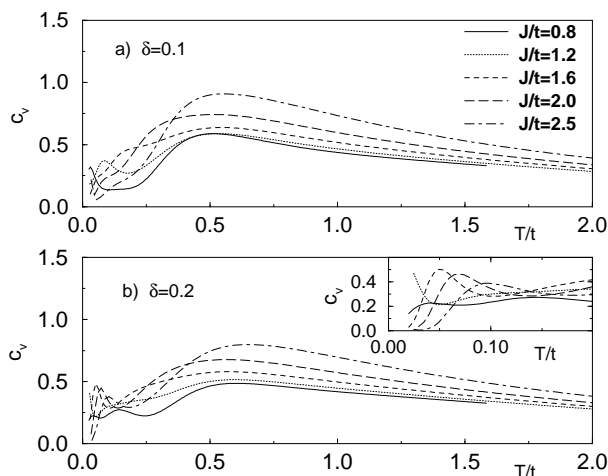


FIG. 6. Specific heat c_v T/t at a) $\delta = 0.1$ and b) $\delta = 0.2$ calculated on a system of $N = 10$. The inset represents the expanded low-temperature region in b).

and financial support of Los Alamos National Laboratory where part of this work was performed. We also acknowledge the support of Slovene-American grant by the Slovene Ministry of science.

TABLE I. The quasiparticle gap Δ_{qp}/J and peak positions T_{qp}/J and T_s/J both presented in units of the Kondo coupling J . Quasiparticle gaps were obtained from the limit $\mu(\delta \rightarrow 0, T \rightarrow 0)$. Spin susceptibilities χ_s can be in the temperature interval $T/J < 0.6$ and for $J/t \leq 2.5$ well fitted to a simple form $\chi_s = C/T \exp(-T_s/T)$ where the effective moment C varies from 0.25 for small J/t to 0.5 at large J/t . Estimated errors where not otherwise specified are within 5%.

J/t ($N = 8$)	Δ_{qp}/J	T_{qp}/J	T_s/J
1.2	0.27	0.31	0.08 ± 0.04
1.6	0.28	0.30	0.13 ± 0.03
2.0	0.30	0.31	0.18 ± 0.03
2.5	0.32	0.31	0.31 ± 0.03
10.0	0.56	0.38	0.47 ± 0.04

J/t ($N = 10$)	Δ_{qp}/J	T_{qp}/J	T_s/J
1.2	0.40	0.49	0.09 ± 0.04
1.6	0.30	0.35	0.15 ± 0.03
2.0	0.29	0.32	0.23 ± 0.03
2.5	0.31	0.32	0.30 ± 0.03
10.0	0.56	0.38	0.47 ± 0.04

-
- [1] J. Jaklič and P. Prelovšek, Phys. Rev. Lett. **77**, 892 (1996); J. Jaklič and P. Prelovšek, cond-mat/9803331.
 - [2] H. Tsunetsugu, M. Sigrist and K. Ueda, Rev. Mod. Phys. **69** 809 (1997).
 - [3] M. Sigrist, H. Tsunetsugu, K. Ueda and T.M. Rice, Phys. Rev. B **46**, 13838 (1992).
 - [4] N. Read, D.M. Newns and S. Doniach, Phys. Rev. B **30**, 3841 (1984).
 - [5] P. Coleman, Phys. Rev. B **29**, 3035 (1984).
 - [6] R. Eder, O. Stoica and G. A. Sawatzky, Phys. Rev. B **55**, R6109 (1997), *ibid* **58**, 7599 (1998).
 - [7] H. Tsunetsugu, Y. Hatsugai, K. Ueda and M. Sigrist, Phys. rev. B **46**, 3175 (1992).
 - [8] S. R. White, Phys. rev. Lett. **69**, 2863 (1992).
 - [9] C.C. Yu and S.R. White, Phys. Rev. Lett. **71**, 3866 (1993).
 - [10] N. Shibata, T. Nishino, K. Ueda and C. Ishii, Phys. Rev. B **53**, R8828 (1996).
 - [11] N. Shibata, J. Phys. Soc. Jpn. **66**, 2221 (1997).
 - [12] X. Wang and T. Xiang, Phys. Rev. B **56**, 5061 (1997).
 - [13] N. Shibata, B. Ammon, M. Troyer, M. Sigrist and K. Ueda, J. Phys. Soc. Jpn. **67**, 1086 (1998).
 - [14] N. Shibata and H. Tsunetsugu, J. Phys. Soc. Jpn. **68**, 744 (1999).
 - [15] N. Shibata and K. Ueda, J. Phys. Condens. Matter **11**, R1 (1999).
 - [16] T. Mutou, N. Shibata and K. Ueda, Phys. Rev. Lett. **81**, 4939 (1999).
 - [17] Z. Wang, X.P. Li, and D.H. Lee, Physica B **199-200**,463 (1994).
 - [18] Z.P. Shi, R.R.P. Singh, M.P. Gelfand and Z. Wang, Phys. Rev. B **51**, 15630 (1995).
 - [19] F.F. Assaad, cond-mat/9904178.